Frontiers in Heat and Mass Transfer

Tech Science Press

DOI: 10.32604/fhmt.2024.047016

ARTICLE

Experimental Investigation of a Phase-Change Material's Stabilizing Role in a Pilot of Smart Salt-Gradient Solar Ponds

Karim Choubani[1,2,*], Ons Ghriss[3], Nashmi H. Alrasheedi[1], Sirin Dhaoui[2] and Abdallah Bouabidi[2]

[1]Department of Mechanical Engineering, College of Engineering, Imam Mohammad Ibn Saud Islamic University, Riyadh, 11432, Saudi Arabia

[2]Mechanical Modeling, Energy & Materials (M2EM), UR17ES47, National School of Engineers of Gabes (ENIG), University of GabesAvenue of Omar Ib-Elkhattab, Zrig, Gabes, 6023, Tunisia

[3]National Engineering School of Gabes (ENIG), Research Laboratory "Processes, Energetics Environment and Electrical Systems", Gabes University, Omar Ibn Kattab Zrig, Gabes, 6029, Tunisia

*Corresponding Author: Karim Choubani. Email: chambanik@yahoo.fr, kElChobani@imamu.edu.sa

Received: 22 October 2023 Accepted: 18 December 2023 Published: 21 March 2024

ABSTRACT

Faced with the world's environmental and energy-related challenges, researchers are turning to innovative, sustainable and intelligent solutions to produce, store, and distribute energy. This work explores the trend of using a smart sensor to monitor the stability and efficiency of a salt-gradient solar pond. Several studies have been conducted to improve the thermal efficiency of salt-gradient solar ponds by introducing other materials. This study investigates the thermal and salinity behaviors of a pilot of smart salt-gradient solar ponds with (SGSP) and without (SGSPP) paraffin wax (PW) as a phase-change material (PCM). Temperature and salinity were measured experimentally using a smart sensor, with the measurements being used to investigate the stabilizing effects of placing the PCM in the solar pond's lower convective zone. The experimental results show that the pond with the PCM (SGSPP) achieved greater thermal and salinity stability, with there being a lesser temperature and salinity gradient between the different layers when compared to a solar pond without the PCM (SGSP). The use of the PCM, therefore, helped control the maximum and minimum temperature of the pond's storage zone. The UCZ has been found to operate approximately 4 degrees above the average ambient temperature of the day in the SGSPP and 7 degrees in SGSP. Moreover, an unstable situation is generated after 5 days from starting the operation and at 1.9 m from the bottom, and certain points have the tendency to be neutral from the upper depths in 1, 3 m of the bottom.

KEYWORDS

Smart salt-gradient solar pond; phase-change material; experimental investigation; stability of solar ponds

Nomenclature

α	Coefficient of thermal expansion (C^{-1}) (±3%)
β	Coefficient of salinity expansion ($m^3.kg^{-1}$) (±3%)
T	Temperature (K)
S	Salinity (%)

E	Stability coefficient ($kg.m^{-1}/\%$)
Z	Height (m)
ρ	Density (kg/m^3) ($\pm 2\%$)

Subscripts

PCM	Phase change material
SGSP	Salinity gradient solar pond without PCM
SGSPP	Salinity gradient solar pond with PCM
UCZ	Upper convective zone
NCZ	Non convective zone
LCZ	Lower convective zone

1 Introduction

Smart energy is becoming increasingly prevalent, both in science and engineering, as well as in daily life. The term "smart energy" does not refer to the nature of the energy itself but rather the ability of systems to optimize the production, distribution, processing, and use of energy while minimizing the environmental impact. Smart energy is therefore often related to notions of green or renewable energy because its technology minimizes energy losses by optimizing the efficiency and stability of energy production and storage systems, such as SGSP.

SGSPs are one of the simplest ways to collect and store solar energy. They contain layers of salt solutions with increasing concentrations and density as the depth increases. When solar radiation (i.e., sunlight) is absorbed, the density gradient inhibits heat in the lower layers from moving upwards through convection. In fact, the temperature can reach 90°C at the bottom of the pond, and it is around the ambient temperature at the top. An SGSP is composed of three zones (see Fig. 1): the lower convective zone (LCZ), the non-convective zone (NCZ), and the upper convective zone (UCZ). The LCZ acts as the collection and storage area, while the UCZ bears all the environmental influences. The NCZ, which is also called the gradient zone, acts as an insulator in limiting the double diffusion of heat and salt from the LCZ to the UCZ. The upper of the system is exposed to solar radiation, which is divided into a reflected part into the air and a transmitted part within the pond. This transmitted part should reach the LCZ to obtain the desired temperature. The LCZ will hold onto the energy absorbed at the bottom of the pond because convective motion will not occur there if the concentration gradient of the NCZ is sufficiently large. Maintaining the NCZ's stability is crucial for optimizing the SGSP's performance, as the SGSP's stability is mostly dependent on its stability.

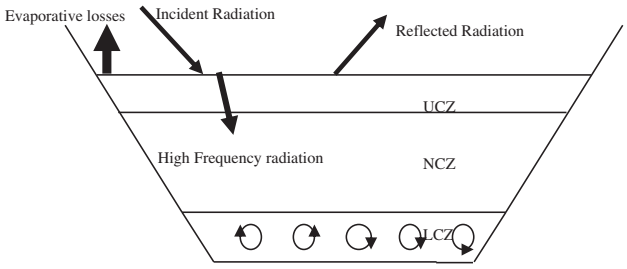

Figure 1: A salt gradient SGSP schematic

One method to enhance the thermal performance of solar energy systems is to use a phase-change material (PCM). Organic phase-change materials (OCPM) have been the basis for developing thermal energy storage materials; Khadiran et al. provided the physio-chemical and thermal properties of encapsulated OPCMs along with a discussion of the various encapsulation strategies used [1]. Meanwhile, based on phase-change material (PCM), Rajesh et al. conducted an experimental study to analyze the thermal performance of various pin fin heat sink designs. In more detail, they investigated a pin fin using n-eicosane and paraffin wax as phase-change materials. An artificial neural network was created to optimize the design, and it was discovered that this worked well for the chosen phase-change materials [2]. In addition to reviewing the use of thermal energy storage materials in buildings, Cao et al. investigated a variety of thermal energy storage materials, such as composite PCMs and microencapsulated PCMs [3]. Sarathkumar et al., meanwhile, sought to minimize the losses in SGSPs by mixing Al_2O_3 nanoparticles with a high heat-absorbing capacity PCM [4]. When comparing an SGSP with a PCM layer to one without, Rghif et al. found that while the amount of heat loss across the saline water-free surface was greater, the temperature and thermal efficiency of the SGSP with the PCM layer were lower. This was due to the Dufour effect and the impact of a PCM layer on the SGSP [5]. Mahfoudh et al., meanwhile, studied the effect on performance of adding salt hydrate PCMs to a small SGSP, with them showing that such an SGSP could be used to produce hot water [6]. Alireza et al. proposed a numerical model to investigate the transfer phenomenon with PCM that they validated with the obtained experimental data. They found that adding PCM allows the enhancement of the SGSP and stabilizes the temperature [7]. Wang et al. numerically and experimentally tested the SGSP with PCM capsules added to the heat storage layer in terms of the pond's thermal performance. They revealed that there is not a significant change in the temperature range between conventional and ameliorated SGPS [8]. Assari et al. applied and compared various stability methodologies to examine the influence of a PCM on the stability of SGSPs and their operating principle, revealing that the pond with the PCM achieved higher thermal and salinity stability and experienced a lower temperature drop during heat extraction when compared to a pond without PCM [9]. Bozkurt investigated the effect of PCMs on improving the insulation of the pond. He determined that using the PCM allowed heat energy to be stored in the SGSP for a longer time [10]. Ihsan et al. investigated the impact of a PCM on the efficiency and applicability of a SGSP, ultimately showing that the use of PCM allows to stabilize the LCZ temperature by the latent heat, thus enhancing the SGSP's efficiency during the colder seasons [11]. Bhartendu et al. discussed the procedures that can be used to decrease the leakage of the PCM during phase transformation. They showed that thermal energy storage PCM can significantly influence the enhancement of solar energy systems. They are characterized by both high energy density and minimum temperature change, which are required for thermal energy storage [12]. Pushpendra et al. evaluated the thermal energy storage performance of Beeswax supported by Bentonite clay and loaded with graphite. They showed the capabilities of Beeswax as a potential alternative to paraffin wax for thermal energy storage. They found that pure Beeswax shows an excellent thermal energy storage capacity of 206.63 J/g (melting) and 203.35 J/g (freezing) at melting and freezing temperatures of 61.60°C and 54.98°C [13]. Poyyamozhi et al. proposed the use of PCM with nano-additives to enhance the efficiency of SGSPs. They showed that the maximum temperature in the LCZ increases for the case of with PCM compared to the case without PCM. In addition, the incorporation of nanoparticles allows an increase in the temperature at 1.3°C compared to the case with PCM [14]. Arulprakasajothi et al. examined the SGSPs system with paraffin wax, additives of nanoparticles and carbon nanotubes. Their experimental investigations found that carbon nanotubes raise the maximum temperature by 26.5% compared to the conventional SGSP. The carbon nanotubes infused PCM increased the heat transfer, heat transfer coefficient, and the heat stored in the saline water by 244%, 713%, and 83.3%, respectively [15]. Apurv et al. studied the performance of solar

thermal storage systems using PCM with the addition of nano additives. They demonstrated that nano-enhanced PCM increases the heat transfer rate and the thermal conductivity in comparison to pure paraffin [16]. Poyyamozhi et al. have investigated the performance of an SGSP with paraffin wax as a PCM and compared it with the addition of nanomaterials such as carbon nanotubes and silver-titanium oxide. They showed that the paraffin wax allows the energy storage to be raised by 7.8%. However, this increase can reach 21.8% and 25% with the use of silver-titanium oxide/paraffin wax and carbon nanotubes/paraffin wax, respectively [17]. Geetesh Goga et al. carried out a series of experiments to analyze the SGSP with PCM and nanoparticles. They revealed that optimum performances were obtained for the case of PCM-containing nanoparticles [18]. Beiki et al. examined the influence of three types of nanoparticles such as SiO_2, Fe_3O_4, and ZnO on the performance of lab scale SGSP. They revealed that the nanoparticles' concentration raises the temperature at the lower zone of the SGSP for all cases. They demonstrated that, for all nanofluids, the bottom layer temperature rose steadily as the concentration of nanoparticles increased. According to experimental data, the SGSP efficiency is enhanced with the addition of all types of nanoparticles [19]. Hamdan et al. (2016) analyze the influence of aluminum oxide Al_2O_3 nanoparticles on the performance of SGSP. It was confirmed that nanoparticles significantly enhance the SGSP performance. This performance can reach 11.3°C for 0.2% concentration of nanoparticles [20]. Colarossi et al. demonstrated an innovative application of PCMs in the LCZ of a small SGSP. They found that after a 6-h heating cycle, the LCZ of the SGSP with PCM is approximately 3°C cooler than the reference example [21]. Wang et al. have studied experimentally the effect of PCM capsule tubes added to an SGSP. They revealed that the temperature difference day-night decreases in the case of SGSP with PCM compared to the conventional SGSP [22]. Amirifard et al. investigated the effect of coupling SGSP with latent heat storage. Two parallel and one series coupling were examined. It was found that the series coupling is more efficient than the parallel coupling [23]. Chaturvedi et al. have reviewed various strategies regarding thermal storage that have been explored further by the addition of PCM. They showed that PCM is one way the solar thermal systems can provide improved performance [24]. Mofijur et al. have examined the usage of PCMs in solar energy storage and utilization, including solar power generation, water heating systems, solar cookers, and solar dryers. They demonstrated that PCMs might be important for storing more energy, which is related to the phase change's latent heat. Furthermore, because of the fixed phase transition temperature, PCMs provide a target-oriented settling temperature. Several factors influence the PCMs' energy storage capability in solar power plants' heat recovery [25]. Al-Obaid developed CFD simulations to examine the effect of various twisted tape configurations on thermal characteristics and flow behavior [26]. Al-Obaidi analyzed the fluid flow and heat transfer characteristics for several tube geometries. He illustrated that the performance evaluation factor ratio of the corrugated tube with different geometrical configurations changed and increased as the corrugated pipe geometrically changed [27]. Varun et al. conducted a review of the several design criteria affecting PCM-assisted systems' performance in 2023. They demonstrated that one generally acknowledged method of improving the thermal performance of energy storage systems is PCM encapsulation. Nonetheless, one of the crucial elements to take into account to guarantee the best possible system performance is the choice of suitable encapsulation shell material and shell geometries [28].

According to the above literature, using a PCM can significantly influence the efficiency of an SGSP. The present study, therefore, investigates the effect of using horizontal cylinders of paraffin wax capsules as a PCM to improve the thermal stability and salinity of a smart SGSP. The variation in temperature and salinity at different solar layers was measured for two similar SGSP prototypes by using a smart sensor, with the results being used as a basis for investigating the stabilizing role of this PCM. Due to the difficulty of determining the stability parameter, most studies on SGSP have not described the stability analysis because the procedure to determine experimentally this parameter is too complex because stability cannot be measured directly from sensor data. In that case, the temperature and density gradients are measured by a sophisticated intelligent sensor in the NCZ, the critical layer in the SGSP, and used to investigate the SGSP performance.

2 Design and Implementation of the Experimental SGSP

This experimental study was conducted on the roof of the College of Engineering building at Imam Mohammad Ibn Saud Islamic University, Riyadh, Saudi Arabia (24.7136° N, 46.6753° E). The experimental SGSP had a total volume of 0.5 m^3 with a truncated conical shape. The cross-sectional area at the bottom and the top of the pond were 0.5 and 1 m^2, respectively, and the total height of the pond was 1 m. To retain the structural stability of the pond and ensure more solar energy per volume, the pond wall was tilted at a 16° inclination, increasing the exposed surface area of the solar basin at the top. In order to prevent heat loss to the surrounding area, the pond's walls were constructed with 3 cm-thick black-colored galvanized iron sheets. These sheets were further insulated by a 5 cm-thick layer of Styrofoam. The complete schematic for the SGSP prototype is shown in Fig. 2. To monitor the temperature and the salinity in the pond, we used the Smart Monitor WIFI SPA Pool Water Quality Meter PH ORP EC PPM (Fig. 3). This innovative device has been designed to help maintain optimal water quality and monitor variations in temperature and water salinity. With its advanced sensors for monitoring pH, ORP, EC, and PPM levels, we could easily keep track of important water parameters in real-time, so there was no guesswork or manual testing required. This device also has built-in Wi-Fi connectivity, allowing us to remotely monitor our experimental SGSP from anywhere with a smartphone or tablet. This sensor measures temperatures from 0°C to 80°C, while for electrical conductivity, it has two mode ranges, namely from 0.0 to 19 mS/cm and from 20.1 to 200 mS/cm. The device connects to a mobile phone application called Tuya through Wi-Fi. Even when we were far away from the SGSP site, we could check the water quality in our pond and adjust the settings as needed with just a few taps on our devices. The Smart Monitor WIFI SPA Pool Water Quality Meter was also incredibly easy to install and use thanks to its intuitive interface and user-friendly applications. We simply attached the sensors to our pond and connected the device to our Wi-Fi network. To measure the temperature and salinity variation at the various layers of the SGSP, this smart monitor was connected to a mechanical system that allowed us to lower and raise the sensor through the pond's depth.

(a) (b)

Figure 2: The experimental smart SGSP (a) and SGSPP (b) prototype

(a) (b)

Figure 3: (a) Smart sensor (b) Tuya smart application interface

3 Filling Techniques for the Pond

Fig. 4 illustrates the preparation and mixing of multiple salt solutions of varying densities in an external reservoir, followed by their transportation to the pond via an electric moto-pump unit driven by a photovoltaic panel. In order to create the LCZ, a solution containing a high concentration of salt (25 percent by weight) was first made and placed at the bottom of the pond, with the height of this zone being 0.3 m. The NCZ consisted of a series of layers with different densities that decreased from bottom to top. To establish this salt gradient zone, we deposited eight layers one above another, on top of the LCZ, starting with the highest concentration at the bottom. Each layer had a thickness of 5 cm and a salinity that was lower than the previous one by a factor of 2%. The first layer of the NCZ was in direct contact with the LCZ. The NCZ acts as an insulator, thus permitting solar radiation to pass through but preventing the heat stored in the bottom layer from moving up. The UCZ, with a height of 0.3 m, was added at the end by using tap water, so it had the lowest density and a temperature closer to ambient temperature. This layer protects the overall system from external and environmental

effects. The pond was filled using a diffuser to minimize the flow velocity and ensure that minimum disturbance occurred. This manual injection diffuser was suspended on a steel cable by a pulley. The hanging cable was connected to a winch so we could adjust the position of the diffuser in the pond. The optimal outlet fluid velocity needed to be chosen to produce lateral mixing at the injection level because an overly fast injection velocity would cause mixing below the injection level. The injection diffuser used for gradient establishment was a double square plate diffuser made from Plexiglas material. The diffuser was moved upward at discrete steps of up to 5 cm. While filling, the SGSP was positioned at an appropriate place and position. During the experimental period, the top of the SGSP was covered by transparent plastic to protect it from external hazards, such as evaporation and contamination. After about a day, the three zones in the SGSP had been constructed, and the system was ready to conduct the experiments.

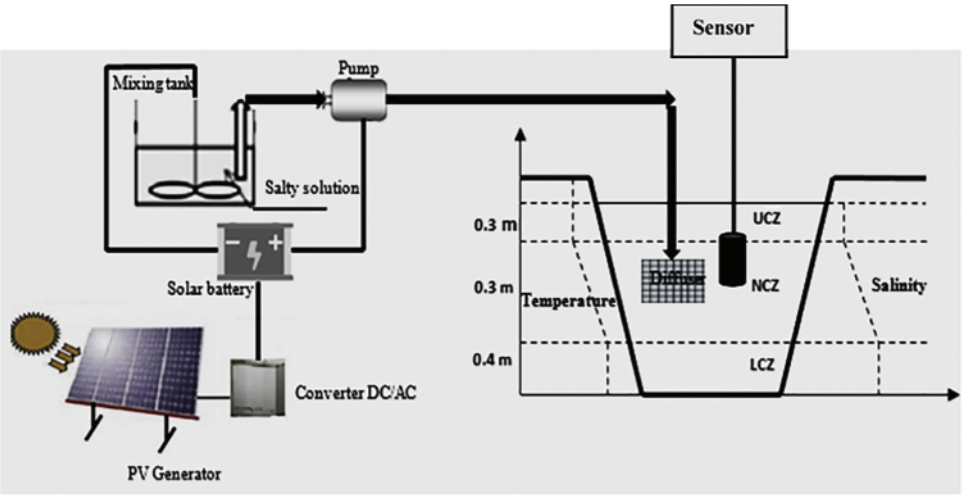

Figure 4: Schematic of salt stratification techniques in our smart salt gradient SGSP prototype

4 Properties of the Paraffin Wax Used in Our Experiments

Paraffin is a family of saturated hydrocarbons. Among all the solid–liquid PCMs, they are the most widely used, especially for low- and medium-temperature applications (i.e., −10°C to 100°C) because they offer the advantage of having latent heat that depends on molar mass and variable phase changes, thus giving more flexibility to choose an appropriate PCM for each application. Paraffin has low thermal conductivity, which limits its applications, and it exhibits a significant volume variation during the phase transition. To increase the conductivity of the paraffin wax used in our experiments, we used 36 horizontal aluminum capsules of paraffin wax, as shown in Fig. 5.

When placed in the bottom layer of the SGSP, these capsules would float upward, so to increase their overall density, we attached them to a small mass that was just dense enough to keep them in direct contact with the bottom of the pond. The properties of the paraffin wax used in our experiments are given in Table 1.

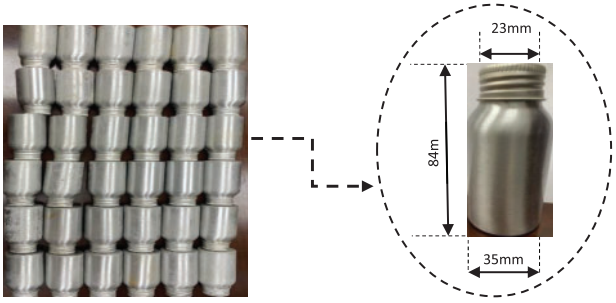

Figure 5: Aluminum capsules of paraffin wax

Table 1: Properties of PCM

Properties	Values
Type of PCM	Paraffin wax
Melting temperature of PCM (°C)	48°C
Density of PCM (g/cm^3)	0.83
Specific heat capacity of PCM (kJ/kg°C)	3.2
Thermal conductivity of PCM (W/mK)	(solid) 0.6; (liquid) 0.56
Height of PCM capsules (cm)	8.4
Diameter of PCM capsules (cm)	3.5
Safety and environmental Performance	Safe and environmental
Volatility	Non-volatile
Cycle times	>10000

5 Monitoring the Stability of the SGSP

Once the stratification is achieved in the pond, instability phenomena are to be expected, mainly in the form of salt diffusing from the bottom of the pond to the surface. These phenomena have been predicted theoretically in the literature for SGSPs and confirmed through experimental studies. In our study, we monitored the local gradient stability with an interest in verifying the instabilities of the salt-gradient layer according to the dynamic instability criterion.

Stability is the main parameter that requires investigation to ensure the proper functioning of an SGSP. Due to the difficulty in determining this parameter, most studies on SGSP have not performed a stability analysis. The method to determine stability is, in general, quite difficult because stability cannot be deduced directly from the sensors that were installed for monitoring SGSP efficiency. Thus, the temperature and concentration gradients, which could be directly and easily measured, were used to monitor the different layers of the system. Stability monitoring took place by monitoring the stability coefficient. This form of monitoring requires the instruments to be capable of measuring the local salinity and temperature gradient at a high spatial resolution with sufficient accuracy, reliability, and ease of operation in order to monitor the internal stability of the pond. For the salt gradient, stability was checked locally between each of the two measurement points. If we consider the linear gradient between two measurement points P_1 (T_1, S_1) and P_2 (T_2, S_2), the stability condition, as suggested by

Alenezi [29] and Montalà et al. [30], can be expressed through Eq. (1).

$$\alpha \frac{\partial T}{\partial z} \leq \beta \frac{\partial S}{\partial Z} \tag{1}$$

Which can also be expressed as:

$$\alpha \frac{\Delta T}{\Delta z} \leq \beta \frac{\Delta S}{\Delta Z} \tag{2}$$

Now, we define the stability coefficient E as follows:

$$E = \frac{\alpha \Delta T}{\beta \Delta S} \tag{3}$$

The stability condition can then be expressed as:

$$E \leq 1 \tag{4}$$

Now, the coefficients of thermal and salinity expansion (α and β) can be calculated though the following equations:

$$\alpha = \frac{\sum_{i=0}^{3} \sum_{j=0}^{3} j A_{i,j} S^i T^{j-1}}{\sum_{i=0}^{3} \sum_{j=0}^{3} A_{i,j} S^i T^j} \tag{5}$$

$$\beta = \frac{\sum_{i=0}^{3} \sum_{j=0}^{3} i A_{i,j} S^{i-1} T^j}{\sum_{i=0}^{3} \sum_{j=0}^{3} A_{i,j} S^i T^j} \tag{6}$$

The values for A_{ij} are given in Table 2 for sodium chloride with a T from 10°C to 100°C, an S from 0% to 26%, and a ρ in kg/m^3.

Table 2: The values of $A_{i,j}$ used to calculate expansion coefficients α and β [30]

j/i	0	1	2	3
0	999.9	7.3624	7.3624×10^{-4}	4.7088×10^{-4}
1	2.5920	-3.3946×10^{-2}	7.7952×10^{-4}	-9.3073×10^{-6}
2	-5.9952×10^{-3}	3.7422×10^{-4}	-1.0436×10^{-5}	1.4816×10^{-7}
3	1.52332×10^{-3}	-9.3860×10^{-7}	3.2836×10^{-9}	4.0083×10^{-10}

The value of Eq. (4) was plotted for each depth over 10 operational days of the SGSP and SGSPP in order to identify where and when the instabilities occur. The use of this equation provided a way to gain a clear view of the system stability and helped us know the location and the timing of the gradient that began the erosion process.

6 Results and Discussion

6.1 Solar Radiation and Ambient Temperature at the Experiment Site

The average measured solar radiation over a year at the collection site in Riyadh, Saudi Arabia is shown in Fig. 6. Peak radiation occurs during the month of June, when it averages more than

7500 Wh/m^2 per day. The least solar radiation occurs from November through February, when it averages less than 5000 Wh/m^2 per day.

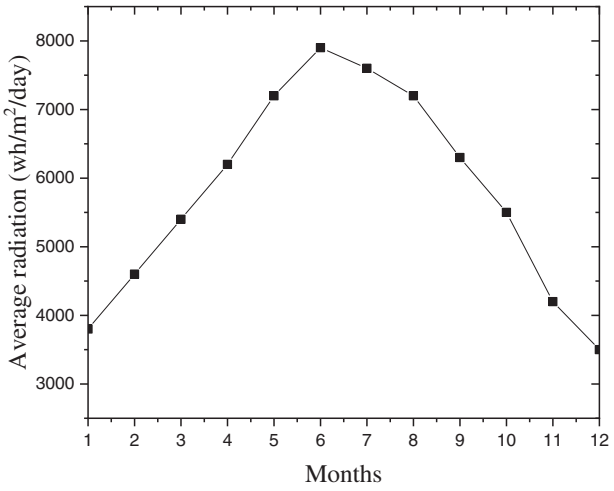

Figure 6: The average radiation, reported monthly, for the city of Riyadh

Peak temperatures occur from June to August, when they exceed 42°C. The lowest temperatures occur during the months of January and December, when they average less than 21°C. The variation in temperature over the year resembles that for solar radiation (Fig. 7).

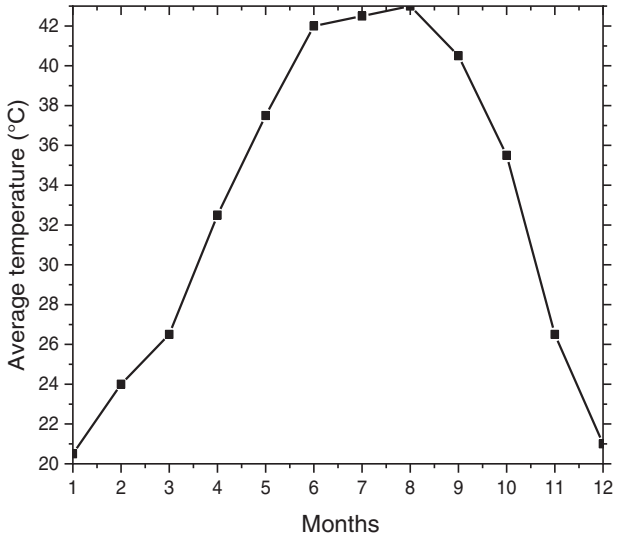

Figure 7: The average temperature, reported monthly, for the city of Riyadh

Fig. 8 shows that the ambient temperature during our experimental period varied between a minimum value of 28.5°C and a maximum value of 44.9°C, with it averaging about 35.3°C. In the same period, the average solar radiation was quasi-constant (Fig. 9) at a value of about 616 W/m^2. The fall in average solar radiation on the seventh day was due to cloudy weather. Fig. 10 shows the variation in solar radiation on the fifth day as an example. As we would expect, peak solar radiation

occurred at mid-day with a value of 958 W/m^2, which is when the highest ambient temperature was also reached.

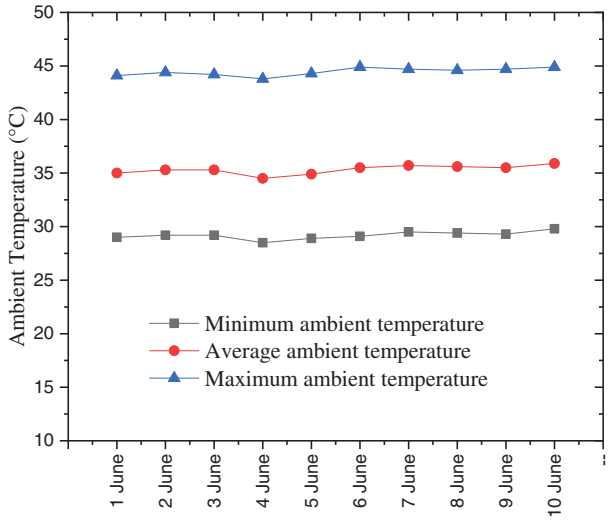

Figure 8: Variation of ambient temperature

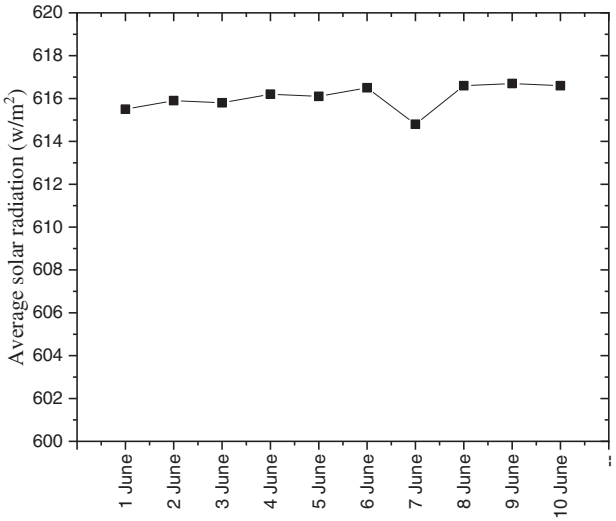

Figure 9: The average solar radiation during SGSPs operation

6.2 Daily Variation in Temperature for Different SGSP Layers

To study the efficiency of our SGSPs and monitor the period of maturation, we measured and recorded the temperature and the salinity of the three zones. Fig. 11 illustrates the daily average temperature data for the UCZ, NCZ, and LCZ layers, as recorded from June 01, 2023 to June 10, 2023 for both the SGSP and SGSPP. A steady rise in temperature can be seen for all pond zones.

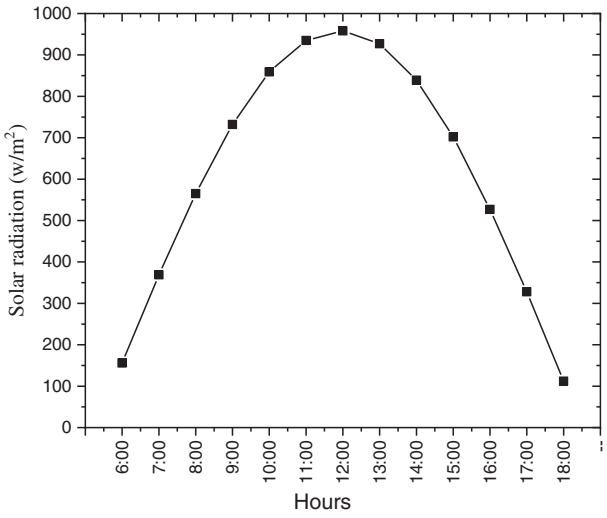

Figure 10: Average solar radiation in the 5th day of the SGSP operation

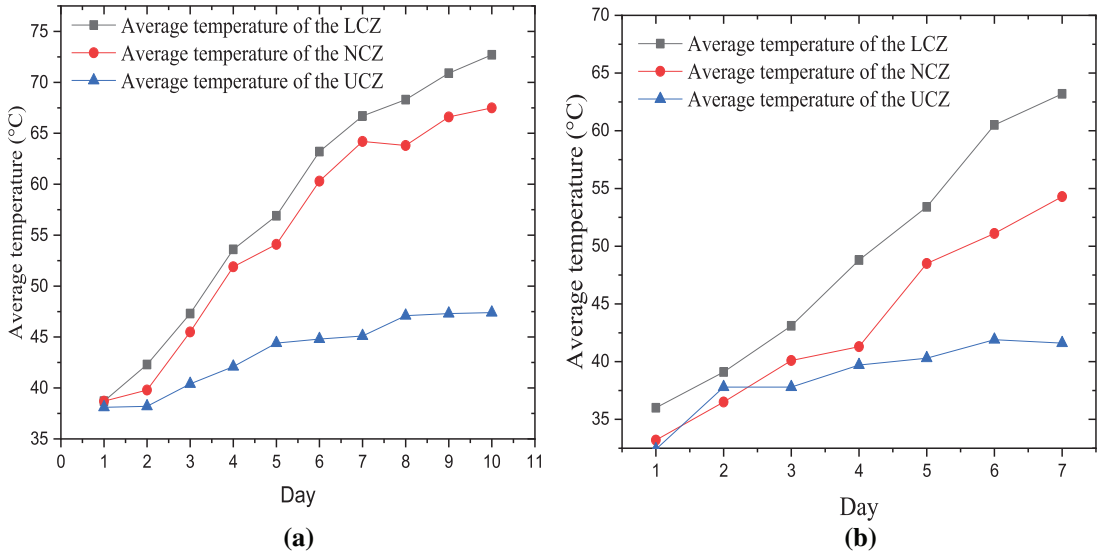

Figure 11: Daily variation of temperature (a) in the SGSP (b) in the SGSPP

The diurnal change in temperature, along with the increase and the decrease in the ambient temperature was least in the UCZ, more in the NCZ, and most marked in the LCZ. However, the highest temperature attained in the UCZ was 47.4°C in the SGSP and 41.6°C in the SGSPP, as shown in Fig. 8, compared with an average recorded ambient temperature of about 40°C (not shown in the figures). Thus, the UCZ was about 4°C hotter than the average ambient temperature of the day in the SGSPP and about 7°C degrees in the SGSP. The obtained results are in very good agreement with experimental data obtained by Poyyamozhi et al. [14]. The temperature variations in the NCZ, as shown in Fig. 11, were more dramatic than they were in the UCZ due to the greater depth of the pond. Nonetheless, because of the LCZ's larger density and deeper location within the pond, daily average temperatures there were roughly 4°C–6°C higher. These outcomes compare favorably to those

of Colarossi et al. [21]. A maximum temperature of about 70°C was reached in the SGSP and 65°C in the SGSPP by the end of the temperature-measurement program. This compares with an ambient temperature of 40°C on the same day, thus implying a temperature increase of about 30°C in the SGSP and 25°C in the SGSPP. This rise is quite significant in terms of the total thermal energy being stored when we consider the total volume of saline water in the UCZ.

6.3 Effect of the PCM on Temperature Variation

Fig. 12 illustrates the temperature variation of the SGSP and SGSPP in the city of Riyadh, Saudi Arabia, as a function of depth for the various days of the experiment. The temperature distribution was measured for ten days without any form of heat extraction from the SGSP. We can see that the temperature in both the UCZ and LCZ is constant because the two layers are considered well mixed in this study, whereas the temperature of the NCZ increases gradually with depth. The LCZ temperature exceeded 50°C after four days of SGSP operation for the SGSP and SGSPP. The highest LCZ temperature exceeded 73°C in the SGSP and 65°C in the SGSPP. As a result of heat transmission between the air and the water's surface, there were very few temperature fluctuations in the UCZ layer compared to ambient temperatures. The temperature ranges of the NCZ fluctuated between 38°C and 65°C in the SGSP and between 38°C and 60°C in the SGSPP. We discovered that the temperature profile of the SGSP was not significantly affected by the PCM layer's use in the absence of any heat extraction from the pond. The PCM only underwent a phase transition to liquid due to the melting temperature brought on by the high temperature of the LCZ layer. Although both the maximum and average temperatures decreased with the PCM, the temperature differences were reduced. Thus, greater thermal and salinity stability could be observed when using the PCM. The temperature profile in the SGSP resembled that of the SGSPP, albeit with a time delay. The three thermal zones in the SGSP (UCZ, NCZ, and LCZ) can clearly be seen in the figure. More specifically, the UCZ was 0.3 m in depth, the NCZ was 0.4 m in depth, and the LCZ was approximately 0.3 m in depth.

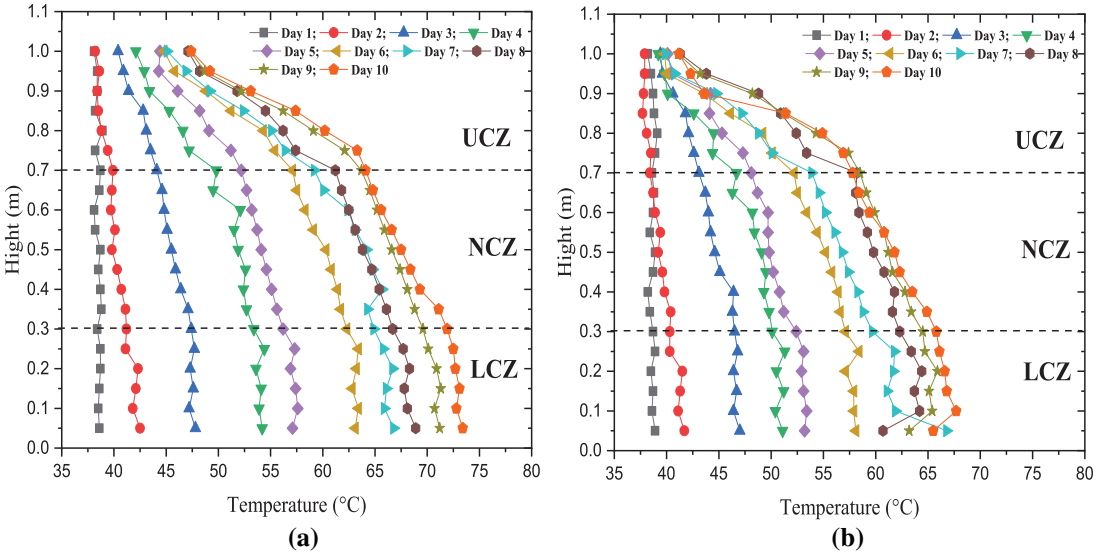

Figure 12: Effect of PCM on temperature variation (a) SGSP (b) SGSPP

The use of PCM helps maintain a more uniform temperature profile within the SGSP, reducing heat losses and improving overall system efficiency. PCM helps regulate the temperature within the

SGSP. During the day, when solar radiation is high, the PCM absorbs excess heat and undergoes a phase change, preventing the water in the SGSP from overheating. During the night or periods of low solar radiation, the PCM releases stored heat, helping to maintain a relatively constant and desirable temperature within the SGSP. This temperature regulation contributes to the stability and performance of the SGSP system.

6.4 Effect of the PCM on Salinity Variation

Fig. 13 shows that the salinity profile was the same in the SGSP and SGSPP. The maximum density in the SGSPP is higher than in the SGSP, which is likely due to the higher temperatures leading to greater solubility of the salt in water. The salinity evolution of the three zones was fairly constant during the experimental period, as can be seen in Fig. 13. Under the influence of external conditions, this response validates the salinity gradient's great stability.

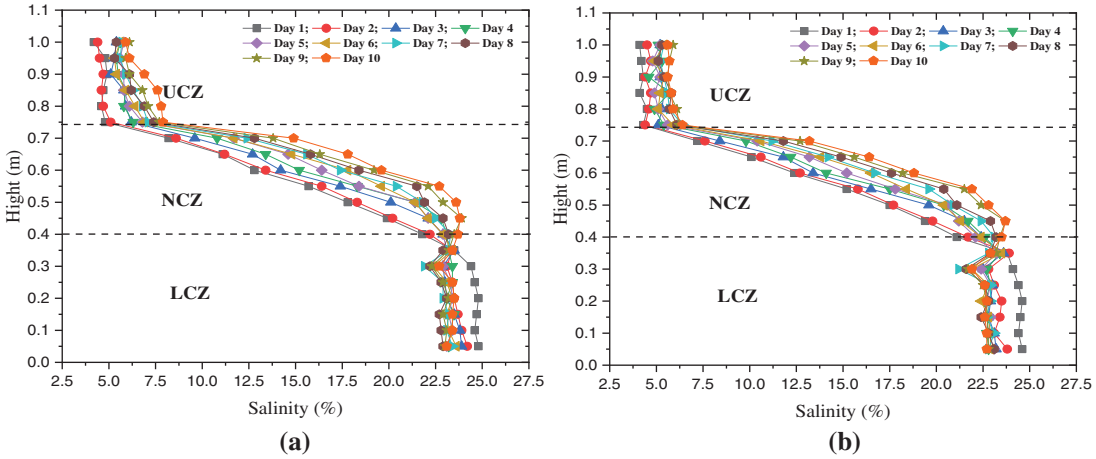

Figure 13: Effect of PCM on salinity variation (a) SGSP (b) SGSPP

The use of PCM allows for a higher energy storage density compared to conventional SGSPs, enabling longer-duration energy storage. The presence of PCM in the SGSP can influence the mixing and stratification patterns of the water. PCM can affect the density and buoyancy of the water, potentially leading to changes in the vertical structure of the pond. This can impact the distribution of salinity within the pond, with variations occurring at different depths.

6.5 Stability Analysis

The salinities were measured at a daily interval, while the stability coefficients for the NCZ were calculated based on the salinity and temperature data. Fig. 14 plots the stability parameter along the NCZ depth, with the various lines representing the stability profile for each level. From this figure, no significant instabilities could be identified. The variation of the stability at each depth can be easily recognized along with the operation of the SGSP. This result allows us to understand the points at different depths that can become unstable. At the beginning, the SGSP appeared stable. However, after five days of operation, a slightly unstable situation was detectable at 1.9 m from the bottom. The system can never return to stability once an unstable condition arises. Fig. 14 illustrates the stability analysis based on the stability parameter for the NCZ depth. These results indicate that the salinity gradient is more significant than the temperature gradient for most of the operational period. Such results confirm the stability condition defined by Eq. (4). In contrast, when the temperature gradient is more

significant than the salinity one, the stability condition is not fulfilled. This investigation confirms a gradient erosion in the lowest part and in the highest layers of the NCZ. This erosion resulted from the different processes that took place where the NCZ met the LCZ. The stability number was calculated to see if it satisfied the temperature profile stability criterion within the NCZ. In principle, this number should be less than 1 to ensure the stability of the NCZ layer.

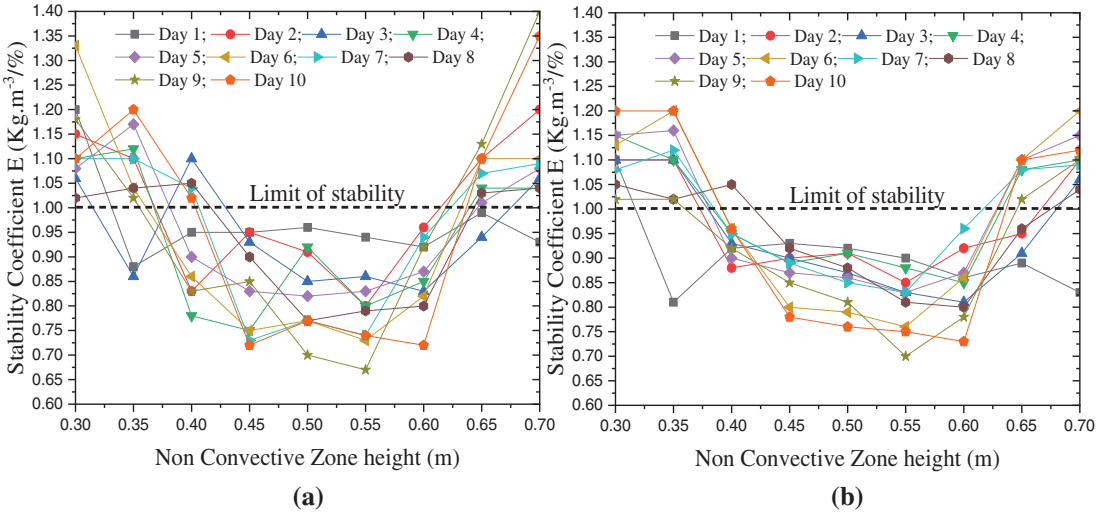

Figure 14: Stability analysis of the non convective zone (a) SGSP (b) SGSPP

According to Fig. 14, no important instabilities were identified. However, some points tended to be neutral (E = 0), mainly at depths greater than 1.3 m from the bottom. It is possible to find instances of small instability at some points, namely at 0.7, 1.3, 1.6, 1.7, and 1.9 m from the bottom. These results are in good agreement with results obtained by Montalà et al. [30].

PCM increases the thermal energy storage capacity of the SGSP. By storing excess heat during periods of high solar radiation, PCM allows for a more continuous and reliable energy supply. This improved energy storage capability enhances the stability of the SGSP by providing a consistent source of thermal energy, even during periods of low solar radiation.

7 Conclusion

The present study investigated the effect of PCM as a solution of energy storage to enhance SGSP efficiency. Our experimental data showed that the maximum temperature value increases in the case of SGSP than in the case of SGSPP. A decrease in the temperature difference was obtained. The minimum temperature was observed to be very close for SGSP and SGSPP. In addition, the SGSP with PCM demonstrated a heat loss that occurred on the free surface, greater than in the case of SGSP without PCM. The SGSP was more affected by the environmental disturbance than the SGSPP. It was found that the UCZ is operating at about 4 degrees above the average ambient temperature of the day in the SGSPP and 7 degrees in the SGSP. The results obtained by the stability analysis based on the salinity and the thermal expansion coefficients are a more useful tool to control the stability of the salinity gradient for the SGSP system. Obtained results showed that after 5 days from starting the operation and at 1.9 m from the bottom, an unstable situation is observed, and the system cannot recuperate its stability again. Moreover, some points tend to be neutral (E = 0), mainly from depths greater than 1.3 m from the bottom. Most studies focused on theoretical analyses of the SGSP stability. Few works

evaluate the stability and validate it with operation data from real SGSP. This study was very promoted in the sense that it explains in a real case the influence of horizontal cylinders of paraffin wax capsules as PCM on the thermal stability and salinity of SGSP. In the case of SGSP without heat extraction from LCZ, using PCM seemed to play the role of porous bodies to stabilize the SGSP stratification.

Acknowledgement: This work was supported and funded by the Deanship of Scientific Research at Imam Mohammad Ibn Saud Islamic University (IMSIU).

Funding Statement: This work was supported and funded by the Deanship of Scientific Research at Imam Mohammad Ibn Saud Islamic University (IMSIU) (Grant Number IMSIU-RG23098).

Author Contributions: The authors confirm contribution to the paper as follows: Conceptualization: Karim Choubani and Nashmi H Alrasheedi; methodology: Karim Choubani; software: Ons Ghriss; validation: Dhaoi Sirin, Bouabidi Abdallah and Karim Choubani; formal analysis: Karim Choubani, Ons Ghriss and Nashmi H Alrasheedi; investigation: Ons Ghriss, Dhaoui Sirin and Karim Choubani; resources: Nashmi H Alrasheedi; data curation: Karim Choubani; writing—original draft preparation: Karim Choubani and Onshriss; writing—review and editing: Nashmi H Alrasheedi and Karim Choubani; visualization: Bouabidi Abdallah; supervision: Karim Choubani; project administration: Karim Choubani; funding acquisition: Nashmi H Alrasheedi and Karim Choubani. All authors have read and agreed to the published version of the manuscript.

Availability of Data and Materials: The data that support the findings of this study are available from the corresponding author, Karim Choubani, upon reasonable request.

Conflicts of Interest: The authors declare that they have no conflicts of interest to report regarding the present study.

References

1. Khadiran, T., Hussein, M. Z., Zainal, Z., Rusli, R. (2015). Encapsulation techniques for organic phase change materials as thermal energy storage medium: A review. *Solar Energy Materials and Solar Cells, 143,* 78–98. https://doi.org/10.1016/j.solmat.2015.06.039
2. Rajesh, B., Balaji, C. (2014). Thermal optimization of PCM based pin fin heat sinks: An experimental study. *Applied Thermal Engineering, 54(1),* 65–77. https://doi.org/10.1016/j.applthermaleng.2012.10.056
3. Cao, L., Di, S., Tang, Y. J., Fang, G. Y., Fang, T. (2015). Properties evaluation and applications of thermal energystorage materials in buildings. *Renewable and Sustainable Energy Reviews, 48,* 500–522. https://doi.org/10.1016/j.rser.2015.04.041
4. Sarathkumar, P., Sivaram, A. R., Rajavel, R., Praveen Kumar, R., Krishnakumar, S. K. (2017). Experimental investigations on the performance of a solar pond by using encapsulated PCM with nanoparticles. *Materials Today: Proceedings, 4(2),* 2314–2322. https://doi.org/10.1016/j.matpr.2017.02.080
5. Rghif, Y., Zeghmati, B., Bahraoui, F. (2021). Modeling the influences of a phase change material and the Dufour effect on thermal performance of a salt gradient solar pond. *International Journal of Thermal Sciences, 1166,* 106979. https://doi.org/10.1016/j.ijthermalsci.2021.106979
6. Mahfoudh, I., Principi, P., Fioretti, R., Safi, M. (2019). Experimental studies on the effect of using phase change material in a salinity-gradient solar pond under a solar simulator. *Solar Energy, 186,* 335–346. https://doi.org/10.1016/j.solener.2019.05.011

7. Alireza, B., Gholi, J., Reza, M., Assarib, H., Tabrizi, B. (2019). Transient modeling for the prediction of the temperature distribution with phase change material in a salt-gradient solar pond and comparison with experimental data. *Journal of Energy Storage, 26,* 101011. https://doi.org/10.1016/j.est.2019.101011
8. Wang, H., Ma, X. M., Zhang, L. G., Zhang, X., Mei, Y. et al. (2020). Numerical and experimental study of effect of paraffin phase change heat storage capsules on the thermal performance of the solar pond. *Energy Exploration & Exploitation,* 1–14. https://doi.org/10.1177/0144598720974160
9. Assari, M. R., Alireza, J. G., Beik, R., Eydi, H., Basirat, T. (2022). Thermal-salinity performance and stability analysis of the pilot salt-gradient solar ponds with phase change material. *Sustainable Energy Technologies and Assessments, 53,* 102396. https://doi.org/10.1016/j.seta.2022.102396
10. Bozkurt, I. (2022). The investigation of using phase change material for solar pond insulation. *Thermal Science, 26,* 1799–1808. https://doi.org/10.2298/TSCI210309185B
11. Ihsan, A. I., Maddahian, R., Maerefat, M. (2023). Investigation of the PCM layer thickness and heat extraction on the thermal efficiency of salt gradient solar ponds. *Case Studies in Thermal Engineering, 45,* 103014. https://doi.org/10.1016/j.csite.2023.103014
12. Bhartendu, M. T., Shailendra, K. S., Pushpendra, K. S. R. (2023). A comprehensive review on solar to thermal energy conversion and storage using phase change materials. *Journal of Energy Storage, 72,* 108280. https://doi.org/10.1016/j.est.2023.108280
13. Pushpendra, K. S. R., Krishna, K. G., Bhaskar, P., Sharma, R. K., Naveen, K. G. (2023). Beeswax as a potential replacement of paraffin wax as shape stabilized solar thermal energy storage material: An experimental study. *Journal of Energy Storage, 68,* 107714. https://doi.org/10.1016/j.est.2023.107714
14. Poyyamozhi, N., Bibin, C. S., Senthil, K., Renugadevi, C. P. (2023). Energy storage investigation of solar pond integrated with PCM and nanoparticles during winter season in Chennai. *Journal of Energy Storage, 73,* 108704. https://doi.org/10.1016/j.est.2023.108704
15. Arulprakasajothi, M., Poyyamozhi, N., Chandrakumar, Dilip Raja, P. N., Yuvarajan, D. (2023). Experimental investigation of salinity gradient solar pond with nano-based phase change materials. *Energy Sources, Part A: Recovery, Utilization, and Environmental Effects, 45(2),* 5465–5480. https://doi.org/10.1080/15567036.2023.2207508
16. Apurv, Y., Maneesh, K. S. (2020). Nanoparticle enhanced PCM for solar thermal energy storage. *Advances in Science and Engineering Technology International Conferences (ASET)*, Dubai, United Arab Emirates. https://doi.org/10.1109/ASET48392.2020.9118287
17. Poyyamozhi, N., Karthikeyan, A. (2022). Comparative energy storage study on solar pond with PCM coupled with different nano particles. *Journal of Mechanical Engineering Science, 236(24),* 11564–11570. https://doi.org/10.1177/09544062221114789
18. Geetesh Goga, G., Afridi, M. S., Mewada, C., Prasad, J., Mohan, R. et al. (2023). Heat transfer enhancement in solar pond using nano fluids. *Materialstoday: Proceedings*. https://doi.org/10.1016/j.matpr.2022.12.238
19. Beiki, H., Soukhtanlou, E. (2019). Improvement of salt gradient solar ponds' performance using nanoparticles inside the storage layer. *Applied Nanoscience, 9(2),* 243–254. https://doi.org/10.1007/s13204-018-0906-6
20. Hamdan, M. A., Al-Qudah, L. A. (2016). Performance improvement of shallow solar pond using nanoparticles. *International Journal of Thermal & Environmental Engineering, 11(2),* 93–98. https://doi.org/10.5383/ijtee.11.02.002
21. Colarossi, D., Principi, P. (2022). Experimental investigation and optical visualization of a salt gradient solar pond integrated with PCM. *Solar Energy Materials and Solar Cells, 234,* 111425. https://doi.org/10.1016/j.solmat.2021.111425
22. Wang, H., Zhang, C. Y., Zhang, L. G. (2022). Effect of steel-wires and paraffin composite phase change materials on the heat exchange and exergetic performance of salt gradient solar pond. *Energy Reports, 8,* 5678–5687. https://doi.org/10.1016/j.egyr.2022.04.021
23. Amirifard, M., Kasaeian, A., Amidpour, M. (2018). Integration of a solar pond with a latent heat storage system. *Renewable Energy, 125,* 682–693. https://doi.org/10.1016/j.renene.2018.03.009

24. Chaturvedi, R., Islam, A., Sharma, K. (2021). A review on the applications of PCM in thermal storage of solar energy. *Materials Today: Proceedings, 43(1),* 293–297. https://doi.org/10.1016/j.matpr.2020.11.665
25. Mofijur, M., Indra Mahlia, T. M., Silitonga, A. S., Ong, H. C., Silakhori, M. et al. (2019). Phase Change Materials (PCM) for solar energy usages and storage: An overview energies. *Energies, 12(16),* 3167. https://doi.org/10.3390/en12163167
26. Al-Obaid, A. R. (2021). Investigation of thermal flow structure and performance heat transfer in three-dimensional circular pipe using twisted tape based on Taguchi method analysis. *Heat Transfer, 51(2),* 1649–1667. https://doi.org/10.1002/htj.22368
27. Al-Obaidi, A. R. (2022). Characterization of internal thermohydraulic flow and heat transfer improvement in a three-dimensional circular corrugated tube surfaces based on numerical simulation and design of experiment. *Heat Transfer, 5,* 4688–4713. https://doi.org/10.1002/htj.22519
28. Varun, G., Ankur, D., Rajat, K., Reji, K., Pandey, A. K. et al. (2023). PCM-assisted energy storage systems for solar-thermal applications: Review of the associated problems and their mitigation strategies. *Journal of Energy Storage, 69*. https://doi.org/10.1016/j.est.2023.107912
29. Alenezi, I. (2012). *Salinity gradient solar ponds: theoretical modelling and integration with desalination (Doctoral Thesis)*. University of Surrey, UK. https://api.semanticscholar.org/CorpusID:129375473
30. Montalà, M., Cortina, J. L., Akbarzadeh, A., Valderrama, C. (2019). Stability analysis of an industrial salinity gradient solar pond. *Solar Energy, 180,* 216–225. https://doi.org/10.1016/j.solener.2019.01.017